

Low-temperature study of the strongly correlated compound $\text{Ce}_3\text{Rh}_4\text{Sn}_{13}$

This article has been downloaded from IOPscience. Please scroll down to see the full text article.

2007 J. Phys.: Condens. Matter 19 386207

(<http://iopscience.iop.org/0953-8984/19/38/386207>)

View [the table of contents for this issue](#), or go to the [journal homepage](#) for more

Download details:

IP Address: 129.252.86.83

The article was downloaded on 29/05/2010 at 04:42

Please note that [terms and conditions apply](#).

Low-temperature study of the strongly correlated compound $\text{Ce}_3\text{Rh}_4\text{Sn}_{13}$

U Köhler¹, A P Pikul^{1,3}, N Oeschler¹, T Westerkamp¹, A M Strydom² and F Steglich¹

¹ Max Planck Institute for Chemical Physics of Solids, Nöthnitzer Strasse 40, D-01187 Dresden, Germany

² Physics Department, University of Johannesburg, PO Box 524, Auckland Park, Johannesburg 2006, South Africa

E-mail: ulrike.koehler@cpfs.mpg.de

Received 31 May 2007, in final form 31 July 2007

Published 29 August 2007

Online at stacks.iop.org/JPhysCM/19/386207

Abstract

Low-temperature results of the thermodynamic and transport properties of polycrystalline $\text{Ce}_3\text{Rh}_4\text{Sn}_{13}$ are presented. The study of the ground-state properties reveals that Kondo interactions become important below 2 K, as evidenced by a large Sommerfeld coefficient and high magnetic resistivity. At 1 K the specific heat exhibits a broad peak that is attributed to short-range magnetic order. Support is given by ac susceptibility measurements. The resistivity and the susceptibility around 80 K are dominated by effects due to the crystal electric field splitting of the Ce^{3+} multiplet. Additionally, clear indications for local vibrations of Sn(2) atoms within the cage-like structure are deduced from an Einstein term in the specific heat. The crystal structure is known to form two atomic cages: one in which the Ce atoms are located; the other containing the Sn(2) atoms. Although strong correlations at low T are present in this system, the thermopower is found to be surprisingly small.

(Some figures in this article are in colour only in the electronic version)

1. Introduction

The search for semiconducting cage compounds with Kondo ions showing strong electronic correlations has been of interest to a considerable number of research groups. The low phonon thermal conductivities, κ_{ph} , often found in filled cage compounds and the large thermopowers, S , typical for Kondo systems are expected to qualify these materials for applications as Peltier coolers [1]. For that purpose the thermoelectric figure of merit, $ZT = S^2T/\rho\kappa$, characterizing

³ Present address: Instytut Niskich Temperatur i Badań Strukturalnych Polskiej Akademii Nauk, P. Nr. 1410, 50-950 Wrocław 2, Poland.

the effectiveness of Peltier cooling as well as of thermal-to-electrical energy conversion needs to attain large values ≥ 1 . Besides high S and low κ_{ph} , semiconducting behavior is desirable in order to lower the electronic thermal conductivity and to avoid low thermopowers, as typically found in good metals.

So far, the main research effort has been put on skutterudites [2] and clathrates [3]. In clathrates, full occupancy of a lattice site by a rare-earth element was only realized for Eu, however, without introducing correlations [4]. An extension of the investigations on materials of different cage-structural types is desirable.

$\text{Ce}_3\text{Rh}_4\text{Sn}_{13}$ crystallizes in the cubic $\text{Yb}_3\text{Rh}_4\text{Sn}_{13}$ structure, which is closely related to the one of skutterudites [5]. It contains two different Sn sites, which were discriminated by Mössbauer spectroscopy [6]. The Rh atoms are situated inside trigonal prisms formed by six Sn(1) atoms. These prisms build a three-dimensional network, which contains two different cages: one is occupied by Ce; the other one by the Sn(2). X-ray diffraction measurements revealed high displacement parameters for the Sn(2) position and suggest the possibility of local vibrations of the Sn(2) atoms inside the cage [6]. This ‘rattling’ is held responsible for the low phonon thermal conductivities found in filled cage compounds. Previous investigations of the resistivity ρ of $\text{Ce}_3\text{Rh}_4\text{Sn}_{13}$ displayed a slight increase from a large room-temperature value of $275 \mu\Omega \text{ cm}$ down to 100 K [6]. A broad maximum is attained in $\rho(T)$ around 100 K, followed by a minimum near 30 K before ρ continues to rise even further towards low temperatures. Concerning the thermopower of $\text{Ce}_3\text{Rh}_4\text{Sn}_{13}$, exploratory measurements [6] showed only a weak temperature dependence in $S(T)$ with values amounting to $\simeq 3 \mu\text{V K}^{-1}$ at room temperature. Nevertheless, the seemingly semiconducting behavior, in combination with the anticipated low κ_{ph} , aroused our interest in scrutinizing the previous thermopower results. Additionally, the absence of magnetic ordering [6] down to 2 K raised the question of the ground state of $\text{Ce}_3\text{Rh}_4\text{Sn}_{13}$. Recent specific heat studies on single crystals showed two successive magnetic transitions at 2 and 1.2 K [7]. The related compound $\text{Ce}_3\text{Ir}_4\text{Sn}_{13}$ undergoes two phase transitions at 2.1 and 0.6 K that were attributed to antiferromagnetic ordering [8–11]. For $\text{Ce}_3\text{Co}_4\text{Sn}_{13}$, specific heat measurements indicate short-range magnetic order below 0.8 K [12]. Magnetic ordering below 10 K was also reported for other isostructural Ce compounds, such as $\text{Ce}_3\text{Os}_4\text{Ge}_{13}$ ($T_N = 6.1 \text{ K}$) [13], $\text{Ce}_3\text{Ru}_4\text{Ge}_{13}$ ($T_N = 6.7 \text{ K}$) [13], and $\text{Ce}_3\text{Pt}_4\text{In}_{13}$ ($T_N = 0.95 \text{ K}$) [14]. These findings stimulated our interest in investigating the ground state of $\text{Ce}_3\text{Rh}_4\text{Sn}_{13}$.

We report on an intensive study of low- T transport and thermodynamic properties of $\text{Ce}_3\text{Rh}_4\text{Sn}_{13}$. The low- T properties are governed by a low-lying Kondo temperature of 2 K. The specific heat exhibits a broad transition at 1 K, which is attributed to antiferromagnetic (short-range?) ordering.

2. Experimental details

Polycrystalline samples of $\text{Ce}_3\text{Rh}_4\text{Sn}_{13}$ were prepared by the arc melting of stoichiometric amounts of the elements and subsequent annealing for two weeks. No signs of minor phases or disorder were detected by x-ray diffraction. However, a diamagnetic contribution to the magnetic susceptibility below 3.6 K indicates traces of elemental Sn of $< 2\%$. As will become evident in the presentation and in the discussion of our results, the principal features and findings for the title compound $\text{Ce}_3\text{Rh}_4\text{Sn}_{13}$ are not affected by this impurity phase. Polycrystalline $\text{La}_3\text{Rh}_4\text{Sn}_{13}$ was also synthesized as a non-magnetic reference compound.

Transport and specific heat measurements in the temperature range from 2 to 300 K were performed in a commercial multi-purpose measurement device (PPMS from Quantum Design). Investigations of the electrical resistivity have been carried out down to 350 mK. Resistivity and

Hall coefficient were measured with a standard four-point ac technique at 31 Hz in fields of up to 9 T. For investigations of the thermopower, a relaxation method with one heater and two thermometers was applied. The specific heat of $\text{Ce}_3\text{Rh}_4\text{Sn}_{13}$ and $\text{La}_3\text{Rh}_4\text{Sn}_{13}$ was measured on the same platform with a 2τ -relaxation-type method. Specific heat measurements in fields for $\text{Ce}_3\text{Rh}_4\text{Sn}_{13}$ were extended down to 100 mK in a dilution refrigerator [15]. Investigations of the dc susceptibility and magnetization were performed between 1.8 and 300 K using a superconducting quantum interference device (SQUID) magnetometer (MPMS from Quantum Design). The ac susceptibility at different frequencies was determined in a dilution fridge between 150 mK and 4 K.

3. Results

The resistivity $\rho(T)$ of $\text{Ce}_3\text{Rh}_4\text{Sn}_{13}$ has been measured for several samples in the temperature range from 350 mK to 300 K. The inset of figure 1 shows the data obtained on the sample with the smallest fraction of elemental Sn, as determined from the change in ρ upon applying a field of 30 mT to suppress superconductivity. Below 3.5 K, data measured in a field of 30 mT are shown, while all the data above this temperature are taken in zero field. Additionally, the resistivity of the non-magnetic reference compound $\text{La}_3\text{Rh}_4\text{Sn}_{13}$ is plotted. $\text{La}_3\text{Rh}_4\text{Sn}_{13}$ exhibits metallic behavior and an intrinsic superconducting transition at 3.8 K [16]. The shoulder in $\rho(T)$ around 60 K is presumably caused by interband scattering, as is often observed for intermetallic compounds of *d*-electron metals [17]. However, considering the crystal structure with the loosely bound Sn(2) atoms, this feature may also be an indication of the enhanced scattering of charge carriers from local vibrations of the Sn. The resistivity of $\text{Ce}_3\text{Rh}_4\text{Sn}_{13}$ remains almost temperature independent at high absolute values, in qualitative agreement with the published data [6] below 200 K. A weak maximum is observed around 50 K. In zero magnetic field below $T \approx 3.5$ K, a small downturn in $\rho(T)$ is found that is caused by the superconducting transition of traces of elemental Sn. The amount of Sn estimated from the magnetic susceptibility of the sample is in the order of 1–2%. In a field of 30 mT, the almost constant resistivity presumably reflects the intrinsic behavior. It is not uncommon in cerium-based compounds with electronic correlations to find a high electronic quasi-particle density of states forming a narrow energy (pseudo) gap near the Fermi level. The electronic transport deriving from these effects can be very sensitive to even spurious amounts of elemental impurities [18]. Therefore, we cannot exclude the possibility that the absolute values of $\rho(T)$ for $\text{Ce}_3\text{Rh}_4\text{Sn}_{13}$ shown in figure 1 might, to some extent, be affected by the presence of a low concentration of Sn-based impurity levels in the sample. For the following measurements the sample with the lowest estimated content of free Sn was used. In the main plot of figure 1 the magnetic contribution to the resistivity, $\rho_{\text{magn}}(T)$, is shown. For that purpose, the phononic part given by the temperature-dependent resistivity of the La compound was subtracted from the resistivity of $\text{Ce}_3\text{Rh}_4\text{Sn}_{13}$. An increasing ρ_{magn} upon decreasing T is deduced, resembling the incoherent Kondo behavior. It is typical for Kondo lattices to show increasingly coherent scattering effects below a few tens of kelvin, resulting in a prominent decrease in $\rho(T)$ below a temperature T^* of the order of the Kondo temperature. Interestingly, $\text{Ce}_3\text{Rh}_4\text{Sn}_{13}$ does not show a temperature dependence of the resistivity of this nature. Qualitatively similar behavior has been found in the tetragonal compound CeRu_4Sn_6 , which is a low-carrier-density system [19]. A common feature in the crystal structures of CeRu_4Sn_6 and $\text{Ce}_3\text{Rh}_4\text{Sn}_{13}$ is that the Ce atoms are in both cases located inside atomic cages of surrounding atoms—a situation that is not conducive to phase-translational coherence in the electronic transport. Instead, the low-temperature part of the resistivity of $\text{Ce}_3\text{Rh}_4\text{Sn}_{13}$ shows a broad maximum around 1 K.

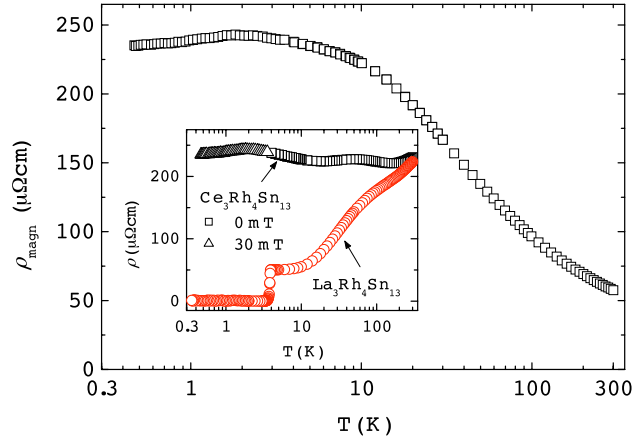


Figure 1. Magnetic part of the resistivity ρ_{magn} of $\text{Ce}_3\text{Rh}_4\text{Sn}_{13}$. Inset: resistivity ρ of $\text{Ce}_3\text{Rh}_4\text{Sn}_{13}$ in $B = 0$ for $T > 3.5$ K, and in 30 mT for $T < 3.5$ K, as well as that of the non-magnetic reference compound $\text{La}_3\text{Rh}_4\text{Sn}_{13}$ in $B = 0$.

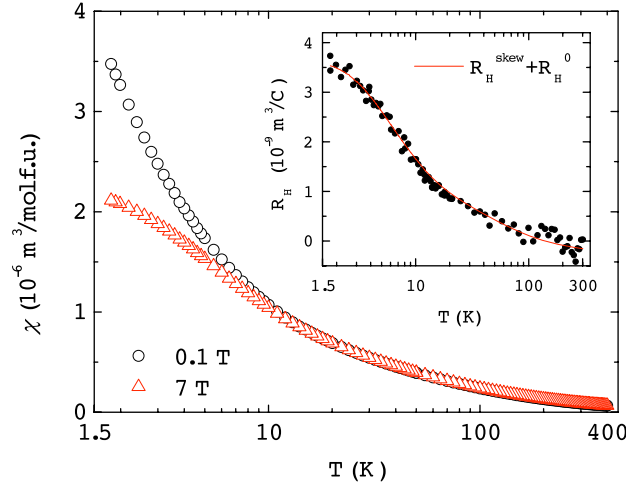


Figure 2. Magnetic susceptibility χ of $\text{Ce}_3\text{Rh}_4\text{Sn}_{13}$ in external fields of 0.1 and 7 T. Inset: Hall constant R_H of $\text{Ce}_3\text{Rh}_4\text{Sn}_{13}$. The fit describes R_H according to $R_H^0 + C_1\rho_{\text{magn}}(T)\chi(T)$.

Figure 2 displays the magnetic susceptibility of $\text{Ce}_3\text{Rh}_4\text{Sn}_{13}$ in external fields of $B = 0.1$ T and 7 T, respectively. In order to estimate the Landau diamagnetic signal due to closed shells, the susceptibility of $\text{La}_3\text{Rh}_4\text{Sn}_{13}$ was also measured. After subtracting the diamagnetic contribution from the susceptibility of $\text{Ce}_3\text{Rh}_4\text{Sn}_{13}$, the data above 60 K can be described by a Curie–Weiss law. A least-square fit yields an effective moment of $2.67 \mu_B$ per Ce, which is close to the free-ion moment expected for Ce^{3+} , and a negative Weiss temperature $\Theta_W = -35$ K, indicating antiferromagnetic correlations. These values are in agreement with previous results [6]. The deviations from the Curie–Weiss law below 60 K may be caused by the existence of a crystal electric field (CEF) splitting. The local symmetry of the Ce site in the structure induces a splitting of the $j = 5/2$ multiplet of the Ce^{3+} ion into three Kramer doublets, as is discussed further below.

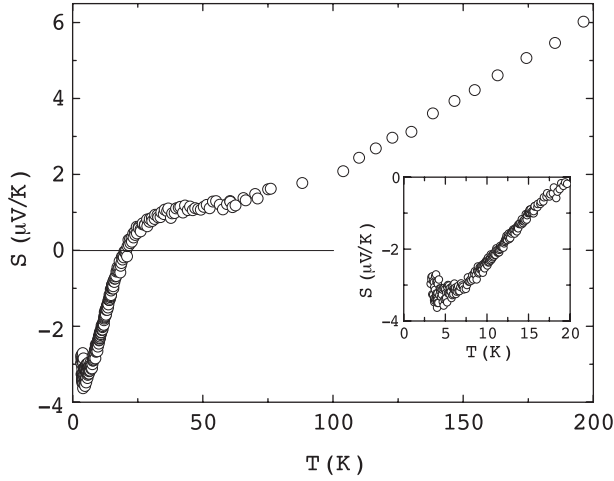


Figure 3. Thermopower S of $\text{Ce}_3\text{Rh}_4\text{Sn}_{13}$. The inset shows the low-temperature part.

The Hall effect was studied in a field of 9 T down to 2 K. The inset of figure 2 shows the Hall coefficient $R_{\text{H}}(T)$. It increases monotonically upon decreasing the temperature and tends to saturate at a constant value at low T . This behavior is in strong contrast to the temperature-independent Hall coefficient R_{H}^0 of single-band metals. The Hall effect of Kondo systems is known to include an anomalous Hall component, $R_{\text{H}}^{\text{skew}}$, which has its origin in the skew scattering from spin-orbit coupling of the f moments. From the point of view that the Hall components act independently, the net Hall coefficient is therefore $R_{\text{H}} = R_{\text{H}}^0 + R_{\text{H}}^{\text{skew}}$. The skew scattering is predicted to follow the temperature dependence of the magnetic contribution to the resistivity ρ_{magn} and the susceptibility χ : $R_{\text{H}}^{\text{skew}} = C_1 \rho_{\text{magn}}(T) \chi(T)$, with C_1 being a constant [20]. A fit to the data is shown as a line in the inset of figure 2. The charge carrier density has been deduced from the normal Hall constant, R_{H}^0 , to be $5 \times 10^{22} \text{ cm}^{-3}$, a value from which overall metallic behavior would be expected for $\text{Ce}_3\text{Rh}_4\text{Sn}_{13}$.

The thermopower $S(T)$ of $\text{Ce}_3\text{Rh}_4\text{Sn}_{13}$ is shown in figure 3. Although the absolute values are somewhat larger than those reported previously [6], no large peak in the thermopower, as is typically observed in Kondo systems and is crucial for thermoelectric applications, is found. At elevated temperatures, S is positive. Around 30 K the thermopower exhibits a shoulder, which may be caused by the CEF splitting of the Ce^{3+} ground state. As scattering from an excited CEF level of Ce^{3+} generates a positive contribution to S with a maximum at approximately $\Delta/3k_{\text{B}}$ [21], the splitting may be estimated to be of the order of $\Delta/k_{\text{B}} = 90$ K. Below 20 K the thermopower becomes negative and goes through a broad minimum around 5 K, where $S = -3.5 \mu\text{V K}^{-1}$.

The specific heats $C(T)$ of $\text{Ce}_3\text{Rh}_4\text{Sn}_{13}$ and $\text{La}_3\text{Rh}_4\text{Sn}_{13}$ above 2 K are shown in figure 4 as $C(T)/T$ versus T . The small anomaly in the specific heat of the Ce compound at 6.5 K is probably caused by magnetic ordering of a foreign phase of Ce oxide [22]. From the entropy released at the transition, the amount of this phase may be estimated to be less than 3%. Above 10 K the $C(T)/T$ behavior of the Ce and La compounds are qualitatively similar. A plot of the specific heat of the La system as $C(T)/T^3$ versus T (upper inset of figure 4) displays a maximum around 10.5 K. Such a behavior is indicative of an Einstein contribution to $C(T)$ [23] with a characteristic temperature of $T_{\text{E}} = 52$ K, which is most probably due to local modes of the Sn(2) atoms. The electronic/magnetic contribution C_{magn} to the specific heat

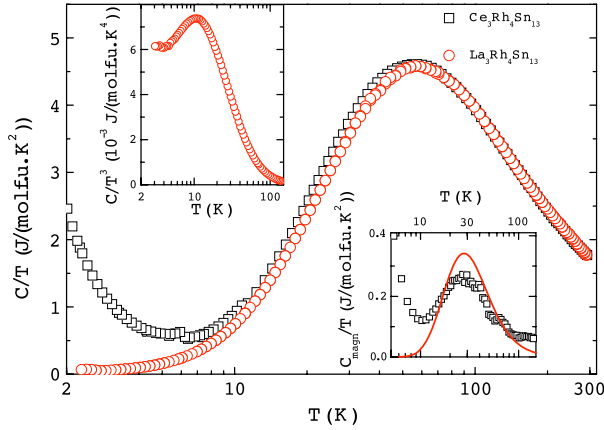


Figure 4. Specific heat divided by temperature C/T versus T for $\text{Ce}_3\text{Rh}_4\text{Sn}_{13}$ and for the non-magnetic reference compound $\text{La}_3\text{Rh}_4\text{Sn}_{13}$. Upper inset: special presentation of the specific heat data of $\text{La}_3\text{Rh}_4\text{Sn}_{13}$ as C/T^3 versus T . In this type of plot, an Einstein contribution generates a maximum near $0.2T_E$. Lower inset: magnetic part of the specific heat C_{magn}/T of $\text{Ce}_3\text{Rh}_4\text{Sn}_{13}$. The fit describes a Schottky contribution of an excited doublet lying at $\Delta/k_B = 90$ K above the ground-state doublet.

of $\text{Ce}_3\text{Rh}_4\text{Sn}_{13}$ is calculated by subtracting the specific heat of $\text{La}_3\text{Rh}_4\text{Sn}_{13}$, which serves as a phononic background. The difference between the data of the Ce and the La compounds is shown as C_{magn}/T in the lower inset of figure 4. The maximum in C_{magn} at 30 K is best described by a Schottky anomaly with an energy splitting of Δ corresponding to $\Delta/k_B = 90$ K between the ground-state doublet and an excited doublet. It is noted that there is only one site provided for Ce atoms in the cubic $Pm\bar{3}n$ crystal structure of $\text{Ce}_3\text{Rh}_4\text{Sn}_{13}$. This ($\bar{4}2m$) site has, however, a tetragonal point symmetry, for which three doublets is an appropriate level-splitting scheme for a Ce^{3+} ion.

The magnetic contribution to the low- T specific heat C_{magn} between 0.1 and 6 K is shown in figure 5. It is dominated by a broad transition with a maximum situated at 1.1 K at values of 3.5 J/(mol Ce K^2). A second transition at 2 K, as found by Ōduchi *et al* [7], was not resolved. By applying a magnetic field, the peak is suppressed in absolute values, but stays at nearly constant temperatures for small fields. In fields above 3 T, on the other hand, the maximum shifts to higher T , keeping the height constant. The low-temperature value of C_{magn}/T for $B = 0$ saturates at a large value of 0.4 J/(mol Ce K^2) typical for a heavy-fermion system.

Figure 6 shows the scaled magnetoresistivity of $\text{Ce}_3\text{Rh}_4\text{Sn}_{13}$, $\rho(B)/\rho(0)$, as a function of the scaled field B/B^* . The scaling of magnetoresistivity in this way follows the $j = 1/2$ case of Schlottmann's description of single-ion Kondo behavior within the Bethe ansatz [24]. For a total angular momentum $j = 1/2$, here assumed to be appropriate for the CEF split ground state of Ce^{3+} in $\text{Ce}_3\text{Rh}_4\text{Sn}_{13}$, an exact solution exists in the Coqblin–Schrieffer class of Hamiltonians. The scaling field $B^*(T)$ is used to obtain both the Kondo moment, μ_K , and the Kondo temperature, T_K , through [25]

$$B^*(T) = B^*(0) + \frac{k_B T}{g\mu_B} = \frac{k_B}{g\mu_K} (T_K + T). \quad (1)$$

From the fits of the scaled magnetoresistivity, we obtain $T_K = 1.6(2)$ K and $\mu_K = 0.050(2)$ μ_B/Ce . This is an exceedingly small value of the Kondo moment when compared to the free-ion value of Ce^{3+} , namely 2.54 μ_B .

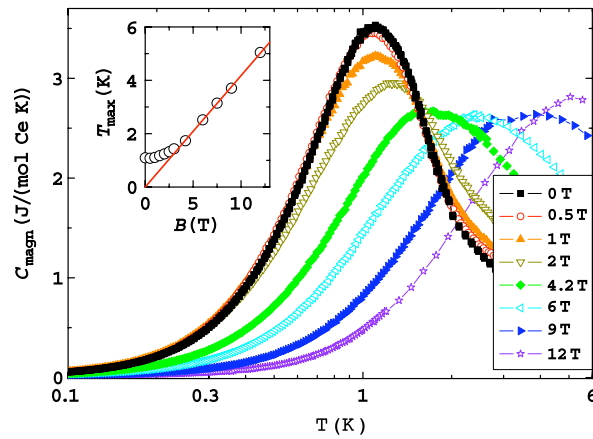


Figure 5. Low- T specific heat C_{magn} of $\text{Ce}_3\text{Rh}_4\text{Sn}_{13}$ for different fields. Inset: T_{max} versus B deduced from the temperature at which the specific heat of $\text{Ce}_3\text{Rh}_4\text{Sn}_{13}$ achieves a maximum. The line is a linear fit through the origin for the data above 4.2 T.

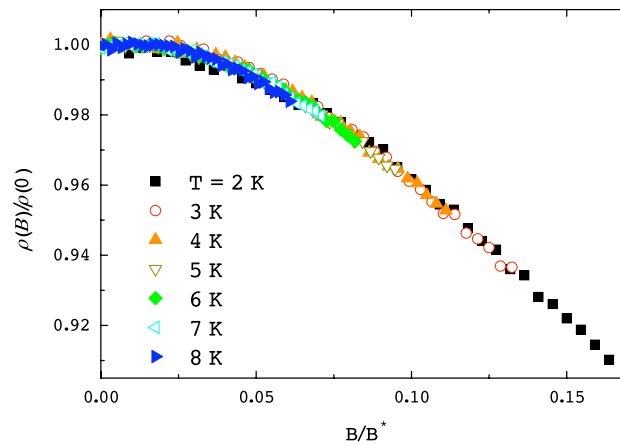


Figure 6. Scaled magnetoresistance $\rho(B)/\rho(0)$ versus the reduced field B/B^* of $\text{Ce}_3\text{Rh}_4\text{Sn}_{13}$ at constant temperatures.

The nature of the broad transition around 1 K is studied further by ac susceptibility measurements χ_{ac} down to 0.1 K at different frequencies of 13, 113, and 1113 Hz at an ac field of $11 \mu\text{T}$. The real part of χ_{ac} , shown in figure 7, exhibits a maximum at 1 K, in accordance with the peak in the specific heat. The structure is very broad and shows no detectable frequency dependence, as would be the case, for example, near a spin-glass transition.

4. Discussion

$\text{Ce}_3\text{Rh}_4\text{Sn}_{13}$ appears to be an interesting compound in view of its ground-state properties and its particular lattice properties. Both resistivity as well as specific heat measurements for the reference compound $\text{La}_3\text{Rh}_4\text{Sn}_{13}$ provide evidence for local vibrations of the loosely bound Sn(2) atoms in the crystal structure. In the specific heat, an Einstein contribution with an Einstein temperature T_E of approximately 50 K is found. Likewise, the shoulder observed in

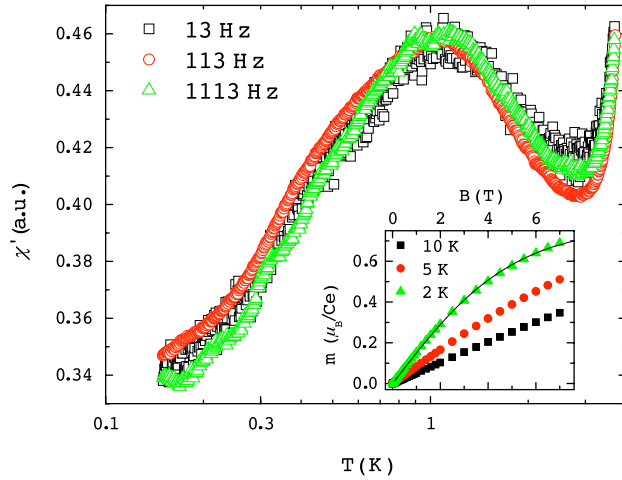


Figure 7. Real part of the low- T ac susceptibility, χ_{ac} , of $\text{Ce}_3\text{Rh}_4\text{Sn}_{13}$ at different frequencies $\nu = 13, 113,$ and 1113 Hz in an ac field of $11 \mu\text{T}$. Inset: effective magnetic moment m per Ce versus B at different temperatures. The solid line is a least-squares fit, as described in the text.

$\rho(T)$ near 60 K may be interpreted in terms of enhanced scattering of charge carriers above T_E . These findings support previous results from x-ray diffraction measurements, which showed large displacement parameters for the Sn(2) position [6]. Evidence for local vibrations of the Sn(2) calls for further investigations of other compounds of the same structural type. The low thermopower as well as its metallic behavior, however, rules $\text{Ce}_3\text{Rh}_4\text{Sn}_{13}$ out as a candidate of high thermoelectric merit. In particular, the Hall effect, though dominated by the anomalous part, indicates metallic behavior: the presumably temperature-independent normal part, R_H^0 , corresponds to $5 \times 10^{22} \text{ cm}^{-3}$, indicating metallic conductivity.

At room temperature, $\text{Ce}_3\text{Rh}_4\text{Sn}_{13}$ acts like an ordinary paramagnetic metal with the full moment of the Ce^{3+} configuration. The corresponding Curie–Weiss behavior in the susceptibility shows deviations only below 60 K which are caused by CEF excitations. Indeed, the specific heat results, cf the lower inset of figure 4, reveal a CEF scheme with a doublet ground state and a first excited doublet at $\Delta/k_B = 90$ K, which is indicated by a Schottky anomaly around 30 K. The entropy confirms the obtained scheme and excludes a quartet state. Thus, the second excited doublet cannot be resolved in the present data on $\text{Ce}_3\text{Rh}_4\text{Sn}_{13}$ and is believed to occur at higher temperatures. The CEF-level energy of the first excited doublet agrees well with recent findings of an inelastic neutron study [26] of $\text{Ce}_3\text{Rh}_4\text{Sn}_{13}$. Features according to the CEF splitting were also observed in the thermopower and resistivity. The thermopower exhibits a shoulder around 30 K, which corresponds to a splitting of approximately 90 K. The magnetic part of the resistivity shown in figure 1 exhibits an increase upon cooling with a change in slope around 10 K and a maximum resistivity at 2 K. The increase in $\rho(T)$ at elevated temperatures is presumably caused by the scattering of the charge carriers off Ce^{3+} Kondo ions in a quasi-quartet state. The rise in $\rho(T)$ below 10 K with smaller slope is attributed to the Kondo scattering from the doublet ground state. No coherence effects are observed at low temperatures, which we ascribe to details of this particular crystal structure. Apparently, coherence effects due to the formation of Bloch waves are prevented by the break-down of translational symmetry. An additional source of the large, almost T -independent resistivity at low T may be strong incoherent scattering processes that occur below $T \approx 1$ K due to short-ranged antiferromagnetic correlations; see below. An

estimate of the Kondo temperature of the CEF doublet ground state is obtained from the magnetoresistance at low T . The data for $1 \text{ K} \leq T \leq 10 \text{ K}$ shown in figure 6 are scaled as $\rho(B)/\rho(0)$ versus B/B^* , with B^* being the Kondo field. According to the analysis of the Bethe ansatz for a Kondo system, the Kondo temperature is 1.6 K. This is confirmed by the analysis of the entropy data: taking as an empirical route that the Kondo temperature amounts to approximately $T_K = 2 \times T(S = 1/2 \ln 2)$ per Ce atom [27], a Kondo temperature of $\approx 2 \text{ K}$ is obtained.

The thermopower of a Ce-based Kondo system typically exhibits a pronounced extremum around the Kondo temperature. However, the minimum in the thermopower of $\text{Ce}_3\text{Rh}_4\text{Sn}_{13}$ lies around 5 K and at a comparably small value of $S_{\min} = -3.5 \mu\text{V K}^{-1}$. It is speculated that those excitations which contribute to the 1 K peak in the specific heat prevent the thermopower attaining larger absolute values at $T = T_K$. The thermopower turns towards positive values at the lowest temperatures studied in this work, and thus it is conceivable that the superposition of both effects leads to the observed small minimum at slightly higher temperatures than T_K .

A broad peak around 1 K with a value as high as $3.5 \text{ J}/(\text{mol Ce K})$ is observed in the magnetic specific heat⁴. A small magnetic field $B \leq 1 \text{ T}$ reduces the absolute values, but has a minor effect on the position of the peak. Intermediate fields shift the peak to higher temperatures. In fields above 3 T the specific heat value at the maximum remains constant and T_{\max} shifts linearly to higher T . A critical field of 3 T at which antiferromagnetism is suppressed has been reported by Ōdachi *et al* [7]. When plotted as $C(T)/T$, the 1 K anomaly is found to broaden in higher fields and show, for $B \geq 4.2 \text{ T}$, the characteristic features of a Gaussian-broadened Schottky anomaly. Plotting the temperature at which C_{magn} exhibits the maximum (cf inset of figure 5), a linear field dependence above 3 T is observed, which extrapolates to $T = 0$ for $B = 0$. The Schottky anomaly is caused by excitations between the Zeeman levels of the ground-state doublet. The slope of the linear-in- B fit corresponds to a magnetic moment of $m_Z = 0.76 \mu_B$, which is in agreement with the expected moment for a Γ_7 doublet ($m_{\Gamma_7} = 0.71 \mu_B$). Further support is obtained from the magnetization measured at 2 K to 7 T, which is shown in the inset of figure 7. The magnetization curve can be described by the Brillouin fit with a saturation moment of $\approx 0.8 \mu_B$. This value is also in accordance with the theoretical value for a doublet ground state.

Evidence for the cooperative magnetic behavior at low temperatures stems from the magnetic measurements. The susceptibility reveals antiferromagnetic correlations with a paramagnetic Weiss temperature of $\Theta_W = -35 \text{ K}$. However, the Kondo screening of the magnetic moments prevents the system from ordering at higher temperatures. In order to unravel the nature of the possible ordering, ac susceptibility measurements at different frequencies were performed at low temperatures; cf figure 7. The data show a broad maximum at 1 K, in accordance with the maximum in specific heat. No frequency dependence could be detected, which excludes the possibility of spin-glass freezing. The broad cusp seen in $\chi_{\text{ac}}(T \simeq 1 \text{ K})$ might result from a disorder-broadened transition, while, on the other hand, short-range antiferromagnetic ordering or spin fluctuations could also be responsible for the observed behavior. The small upward shift of the transition temperature in low fields (cf figure 5) is presumably caused by the interplay between reducing the antiferromagnetic transition temperature and the suppression of the Kondo screening. Since the Kondo temperature is small, a small field suppresses the screening and stabilizes the moment that orders at 1 K. Due to the larger moment, which increases with field, the ordering temperature is effectively shifted to higher temperatures. Once the Kondo effect is completely destroyed at

⁴ Recent specific heat studies on single crystals have shown a peak with identical height and broadness. It is therefore believed to be intrinsically broadened.

larger fields, the ordering is lost and only the Zeeman split CEF doublet ground state contributes to the specific heat.

5. Conclusion

The low- T properties of the compound $\text{Ce}_3\text{Rh}_4\text{Sn}_{13}$ have been studied extensively. A CEF scheme with a ground-state doublet and a first excited doublet at $\Delta/k_B = 90$ K has been determined by means of specific heat measurements. The magnetic resistivity increases upon cooling due to the Kondo scattering at Ce^{3+} ions with a CEF split $4f$ state. The Kondo temperature of the lowest-lying CEF doublet was deduced to be $T_K \simeq 2$ K by analyzing both the magnetoresistance and the magnetic entropy. The present state of investigation into $\text{Ce}_3\text{Rh}_4\text{Sn}_{13}$ points toward a ground state that is probably of short-range antiferromagnetic order, and with a transition that may be broadened in addition by disorder effects. In applied magnetic fields the Kondo screening becomes suppressed, which leads to a shift of the transition temperature since the magnetic moment rises in field. At fields $B \geq 4.2$ T the specific heat exhibits a Schottky anomaly, which marks the excitations between the Zeeman levels of the CEF doublet ground state.

Neutron diffraction experiments, as well as muon-spin-relaxation studies, are highly desirable to clarify the nature of the magnetic ordering and the ground state in $\text{Ce}_3\text{Rh}_4\text{Sn}_{13}$.

Acknowledgments

Fruitful discussions with M Baenitz are acknowledged. A M Strydom gratefully acknowledges the hospitality of the Max Planck Institute for Chemical Physics of Solids in Dresden. A P Pikul is indebted to the Alexander von Humboldt Foundation for financial support.

References

- [1] Paschen S 2006 Thermoelectric aspects of strongly correlated electron systems *CRC Thermoelectrics Handbook* ed D M Rowe (Boca Raton, FL: CRC Press) chapter 15 and references therein
- [2] Sales B C *et al* 1996 *Science* **272** 1325
- [3] Nolas G S 2001 *Semicond. Semimet.* **69** 255
- [4] Paschen S *et al* 2001 *Phys. Rev. B* **64** 214404
- [5] Remeika J P *et al* 1980 *Solid State Commun.* **34** 923
- [6] Niepmann D *et al* 2001 *Z. Naturf.* b **56** 1
- [7] Ödücü Y *et al* 2007 *J. Magn. Magn. Mater.* **310** 249
- [8] Sato H *et al* 1993 *Physica B* **186–188** 630
- [9] Takayanagi S *et al* 1994 *Physica B* **199/200** 49
- [10] Israel C *et al* 2005 *Physica B* **359–361** 251
- [11] Nagoshi C *et al* 2005 *Physica B* **359–361** 248
- [12] Cornelius A L *et al* 2006 *Physica B* **378–380** 113
- [13] Segre C U *et al* 1981 *Ternary Superconductors* ed G K Shenoy, B D Dunlap and F Y Fradin (Amsterdam: North-Holland) p 243
- [14] Hundley M F *et al* 2001 *Phys. Rev. B* **65** 024401
- [15] Wilhelm H *et al* 2004 *Rev. Sci. Instrum.* **75** 2700
- [16] Hodeau J L *et al* 1982 *Solid State Commun.* **42** 97
- [17] Calandra M and Gunnarsson O 2002 *Phys. Rev. B* **66** 205105
- [18] Nakamoto G *et al* 1995 *J. Phys. Soc. Japan* **64** 4834
- [19] Strydom A M *et al* 2005 *Physica B* **359–361** 293
- [20] Fert A and Levy P M 1987 *Phys. Rev. B* **36** 1907
- [21] Bhattacharjee A K and Coqblin B 1976 *Phys. Rev. B* **13** 3441

- [22] Sereni J G 1991 *Handbook on the Physics and Chemistry of Rare Earths* vol XV, ed K A Gschneider Jr and L Eyring (Amsterdam: North-Holland) chapter 98
- [23] Lawless W N 1976 *Phys. Rev. B* **14** 134
- [24] Schlottmann P 1983 *Z. Phys. B* **51** 223
- [25] Batlogg B *et al* 1987 *J. Magn. Magn. Mater.* **63/64** 441
- [26] Adroja D T *et al* 2007 *Proc. Int. Conf. Strongly Correlated Electron Systems (Houston, Texas, USA)*; *Physica B* at press
- [27] Desgranges H-U and Schotte K D 1982 *Phys. Lett. A* **91** 240